Water-Induced Rearrangement of $Ca(OH)_2$ (0001) Surfaces Reacted with SO_2

M. Bausach, M. Pera-Titus, C. Fite, F. Cunill, J.-F. Izquierdo, J. Tejero, and M. Iborra
Chemical Engineering Dept., University of Barcelona, 08028 Barcelona, Spain

DOI 10.1002/aic.10907
Published online June 19, 2006 in Wiley InterScience (www.interscience.wiley.com).

AFM imaging and EDS microanalyses provide evidence of the reorganization of single-crystal $Ca(OH)_2$ (0001) surfaces attacked by SO_2 at low temperature when exposed to water vapor in such a way that larger product features are formed from the aggregation of smaller ones. This product rearrangement induced by water vapor might provide a new accessible $Ca(OH)_2$ surface for further reaction with SO_2, which might account for the general observation reported in the literature that water vapor exerts a substantial influence on the ability of commercial hydrated lime to retain SO_2 in flue gas desulfurization (FGD) technologies. A reaction mechanism consistent with the experimental observations and with its kinetic implications is discussed. © 2006 American Institute of Chemical Engineers *AIChE J,* 52: 2876–2886, 2006
Keywords: AFM, SO_2, calcium hydroxide, reaction mechanism, water vapor

Introduction

The reaction between hydrated lime [that is, $Ca(OH)_2$] and SO_2 at low temperature (<450 K) has received much attention in the past decades because it constitutes one of the fundamental reactions involved in flue gas desulfurization (FGD) technologies implemented in industrial combustors. The overall reaction that takes place in these processes can be described by the following equation[1]:

$$Ca(OH)_{2(s)} + SO_{2(g)} \xrightarrow{H_2O_{(v/ads)}} CaSO_3 \cdot (1/2)H_2O_{(s)} + (1/2)H_2O_{(v/ads)} \quad (1)$$

where part of calcium sulfite can be oxidized to calcium sulfate if oxygen (O_2) is present. Although the experience gathered in this field until now clearly reflects that water vapor is the most relevant operational variable on both the ability of $Ca(OH)_2$ to retain SO_2 and on the kinetics of the process,[2-6] the reaction mechanism and how water vapor takes part in it still constitutes an unclear and intricate issue.

The outstanding effect exerted by water vapor on the reaction seemingly indicates that water physically adsorbed on the reagent surface might play a key role in the reaction. According to the BET (Brunauer–Emmett–Teller) classification, the adsorption of water vapor on $Ca(OH)_{2(s)}$ follows a Type II isotherm,[7,8] which involves the formation of a water multilayer at high relative humidity (RH). In particular, the surface coverage of water on $Ca(OH)_2$ at 343 K is >2.0 for RH > 70%.[7] The physical state of water thin layers at a molecular level seems to be relevant to understand and describe the implications of water in the reaction. Although to our knowledge water thin films on $Ca(OH)_{2(s)}$ have not yet been described, some studies can be found in the literature concerning their characterization on $NaCl_{(s)}$. These studies might provide valuable information, especially at high surface coverage, where water interactions might be less influenced by the substrate. The results found in several recent studies[9-11] sustain that, at ambient temperature (283–298 K) and for water partial pressures in the range 0–2.5 kPa, water is adsorbed on NaCl (100) planes forming a "liquid-like" thin film, that is, the bonding pattern of the layer is characterized by an isotropic hydrogen bonding network resembling that in liquid water. In these conditions, Na^+ and Cl^-

Correspondence concerning this article should be addressed to M. Bausach at mbausach@ub.edu.

ions are expected to be drawn from the crystalline lattice into the water layer.[9]

Several attempts have been made to describe the role of adsorbed water in the mechanism of the reaction under study. Some authors[12,13] suggested the formation of a water multilayer at high RH that could allow a partial dissolution of the $Ca(OH)_2$ surface to form a Ca^{2+} and HO^- ionic solution through which SO_2 could diffuse and react. A similar mechanism was also proposed by Beruto and Botter[8] to explain the effect of water vapor on the reaction between $Ca(OH)_2$ and CO_2. Another approach[7] argued that SO_2 molecules could be stabilized on the reagent surface by the formation of some hydrated complexes that could further react with $Ca(OH)_{2(s)}$. Eventually, other researchers[14] hypothesized that, as the reaction proceeds, a continuous $CaSO_3 \cdot (1/2)H_2O_{(s)}$ product layer might be formed onto the reagent surface, through which $SO_{2(g)}$ molecules might diffuse to come into contact with the unreacted solid for further reaction. According to this latter mechanism, the total amount of adsorbed water could act modifying either the physical characteristics of the product layer or the SO_2 diffusivity, which would be responsible for the dramatic enhancement of the reactivity of the system. On the other hand, other product morphologies (such as "cluster-like") could also promote the accessibility of SO_2 to attain the still unreacted $Ca(OH)_2$ reagent, thus leading to higher SO_2 uptake. In case different product morphologies were obtained at different RH values, this could account for the strong dependency of the reactivity of the system with the RH.[4] However, in a previous study done using atomic force microscopy (AFM), it was shown that the sulfite product is arranged on the surface forming "needle-like" features irrespective of the RH at which the reaction takes place.[15]

Regarding the kinetics of the desulfurization reaction, experimental data obtained in our laboratory were successfully fitted to a deactivation model (DM) combined with an outward ionic solid-state diffusion step (ISCM).[16,17] This model takes into account the reduction of the active surface of $Ca(OH)_2$ while the reaction progresses and an outward solid-state diffusion of hydrated Ca^{2+} and HO^- ions from the inner $Ca(OH)_2$/$CaSO_3 \cdot (1/2)H_2O$ to the outer $CaSO_3 \cdot (1/2)H_2O$/gas interface. In this article we provide a new insight into the reaction under study by imaging the evolution of some $Ca(OH)_2$ (0001) surfaces attacked by SO_2 with tapping mode (TM)–AFM after exposure to a humid atmosphere. A reaction mechanism consistent with both the AFM observations and our kinetic model (DM-ISCM) is also discussed.

Experimental

Synthesis of $Ca(OH)_2$ single crystals

$Ca(OH)_2$ single crystals were prepared in our laboratory by means of the so-called diffusion method.[18] Two precursor aqueous solutions of $CaCl_2$ and NaOH (30 and 24 g, respectively, in 100 mL of distilled water) were prepared in two different glass beakers, by adding a small amount of $Ba(OH)_2$ to the latter to retain the CO_2 absorbed in the course of the crystallization process by the precipitation of $BaCO_3$. Both beakers were immersed in a larger one, and distilled water was added until the water level reached about 1 cm over them, so that the involved ions (Ca^{2+} and HO^-) could come into contact for further crystallization. Finally, the crystals were filtered, washed with methanol, and dried overnight at 383 K. With this method, single crystals up to 2–5 mm in size were obtained after 4 weeks. According to the X-ray diffraction (XRD) patterns (not shown here), they showed high crystallinity and purity. The crystals were hexagonally shaped, according to the hexagonal space group $P\bar{3}m1$[19] at which $Ca(OH)_2$ crystallizes.

Table 1. Lattice Parameters and Atomic Distances of $Ca(OH)_2$

Property	Value[18–20] $Ca(OH)_2$ crystal
Lattice parameters (Å)	
A	3.5918
B	3.5918
C	4.9063
Atomic distances (Å)*	
O—H	0.984, 2.665
Ca—O	2.371
	3.592 (in basal plane)
O—O	3.333 (the other edges of the CaO_6 octahedron)
	3.095 (the H-containing O_4 tetrahedron)
SO_2 molecule	
Dipolar moment (D)	1.59 ± 0.01
S—O distances (Å)	1.432 ± 0.001
O—S—O bond angle (°)	119.54

*Determined by neutron diffraction.

The main data concerning the lattice parameters and atomic distances of the $Ca(OH)_2$ unit cell are summarized in Table 1. In addition, a unit cell of the lattice and a projection on the (0001) plane are depicted in Figure 1. As can be seen in Figure 1b, the calcium ions lie in the (0001) planes and those containing the hydroxyl ions are parallel to them at a position 0.233c and −0.233c. As a result, hydroxyl ions lie alternately above and below the planes containing the calcium ions (see Figure 1c). The layers are held together by weak secondary forces occurring between the neighboring HO^- ion layers.

Reaction of $Ca(OH)_2$ single crystals with SO_2

In the beginning of each experiment, one $Ca(OH)_2$ single crystal was cleaved with a sharp blade to generate a (0001) plane and the resulting cleaved crystal was fixed on a Teflon® base. The fresh surface was explored by TM-AFM to assess its smoothness and uniformity. A TM-AFM image of a freshly cleaved $Ca(OH)_2$ (0001) plane is shown in Figure 2. As can be seen, the surface is quite regular with very low roughness [root mean square (RMS) roughness (or simply, RMS) < 0.3 nm]. The smooth terraces are interrupted by steps of height about 0.5 nm, which roughly corresponds to the lattice parameter c of the $Ca(OH)_2$ unit cell (see Table 1).

The experimental setup for carrying out the reaction between the cleaved $Ca(OH)_2$ single crystals and SO_2 is schematically drawn in Figure 3. The equipment consisted of a glass reactor (R) immersed in a thermostatic bath, a feeding system, and two valves (V) at the inlet and outlet of the reactor that allowed its isolation with a desired atmosphere (composition, pressure, RH, and temperature) during each experiment. The gas feed was generated by feeding the appropriate amount of pure gases (SO_2 and N_2) from pressurized gas cylinders and regulated by

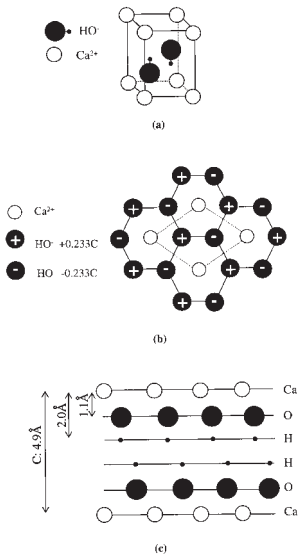

Figure 1. Hexagonal lattice of $Ca(OH)_2$.

(a) Unit cell. (b) Projection on the (0001) plane. (c) View of the layered structure.

means of mass flow (MF) controllers (Models 5850S, Brooks Instruments B.V., Veenendaal, The Netherlands). The steam feed was obtained by using a controlled evaporator mixer (CEM; Bronkhorst Hi-Tech, Ruurlo, The Netherlands) equipped with a liquid mixing valve (MV) to control the water flow rate. The relative pressure in the reactor was controlled by means of a manometer (M; range 0–1 $\pm$ 0.05 bar). To prevent the system from any water condensation, all the pipes were wiped using an electric resistance (ER).

The crystals were placed immediately in the reactor just after being cleaved. The desired flows of water vapor, SO_2, and N_2 were supplied to the reactor and after 1 min it was isolated and the total pressure was fixed at a value of 120 kPa to maintain the RH inside the reactor at a controlled value. The reactor was kept at 313 K and 5500 ppm of SO_2 concentration in N_2 at fixed RH values during the reaction time (30 min), after which it was fed with pure N_2 to stop the reaction. Then, the reactor was isolated in a dry N_2 atmosphere and removed from the system. The reacted crystal was kept inside the reactor until the AFM analyses were performed to prevent the reacted surface from any further change arising from the action of atmospheric humidity.

Humidification of the reacted samples

After the reaction with SO_2, the crystal samples were submitted to a humidification step by means of three different procedures:

Procedure A: Short-Time Humidification at High Water Vapor Pressure. The reacted crystals were again placed in the reactor at 313 K and 80% RH (water partial pressure: 5.9 kPa) for 2 h and after this period the same surface region was newly imaged.

Procedure B: Long-Time Humidification at Room Conditions. The reacted crystals were left at room conditions for some days. The same surface region was explored several times until no significant changes were observed. The RH and temperature showed values in the range 60–80% and 288–298 K, respectively, during the exposure (water vapor pressure: 1.4–1.9 kPa).

Procedure C: In Situ Humidification. The reacted crystals were humidified and simultaneously imaged (one image acquired every 2.5–3.0 min). Once the crystal samples were placed onto the AFM support, the AFM scanning unit was placed inside a controlled-humidity chamber. First, dry N_2 circulated through the chamber until the RH was $<15\%$ (<0.4 kPa) (about 5 min required) and then the AFM imaging started. Subsequently, the chamber was humidified by bubbling dry N_2 in liquid water, achieving a 75% RH (2.0 kPa) at room temperature (293–298 K) after about 10 min. The RH was kept at 75% RH for a period of 90 min during which the surface was continuously monitored.

In addition, to ensure that any morphological change on the reacted surfaces was attributed only to the sulfite product [that is, $CaSO_3 \cdot (1/2)H_2O_{(s)}$] instead of the reagent, some preliminary experiments were performed with an unreacted cleaved $Ca(OH)_2$ single crystal with further humidification according to procedures B and C. Moreover, to ensure that any change in surface morphology arose from the effect of water, some reacted samples were kept in a desiccator containing P_2O_5 (Sigma-Aldrich Chemie GmbH, Munich, Germany) as desiccant agent at room temperature (292–299 K) for 7 days and under vacuum (<4 kPa), and afterwards they were newly imaged by AFM.

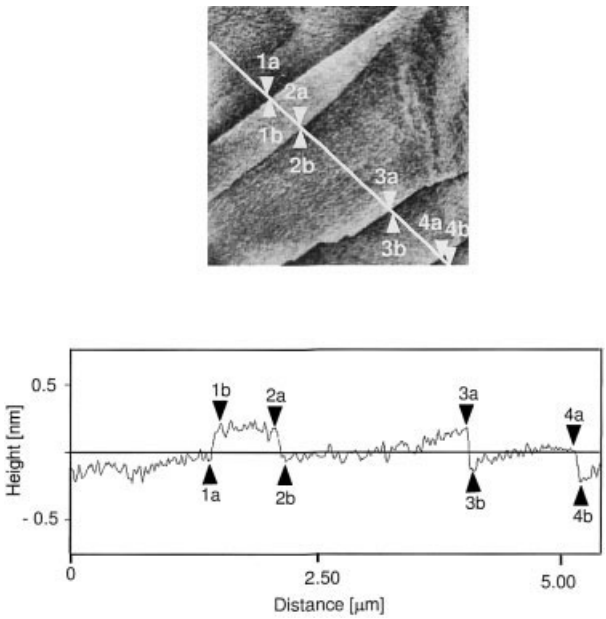

Figure 2. TM-AFM image of a freshly cleaved single-crystal $Ca(OH)_2$ (0001) surface.

(a) 4×4 μm^2 image. (b) Profile, where the presence of steps, whose height corresponds to the lattice parameter c of the $Ca(OH)_2$ unit cell, can be seen. Step heights: 1a–1b: 0.501 nm; 2a–2b: 0.474 nm; 3a–3b: 0.594 nm; 4a–4b: 0.499 nm. Rms: 0.195 nm.

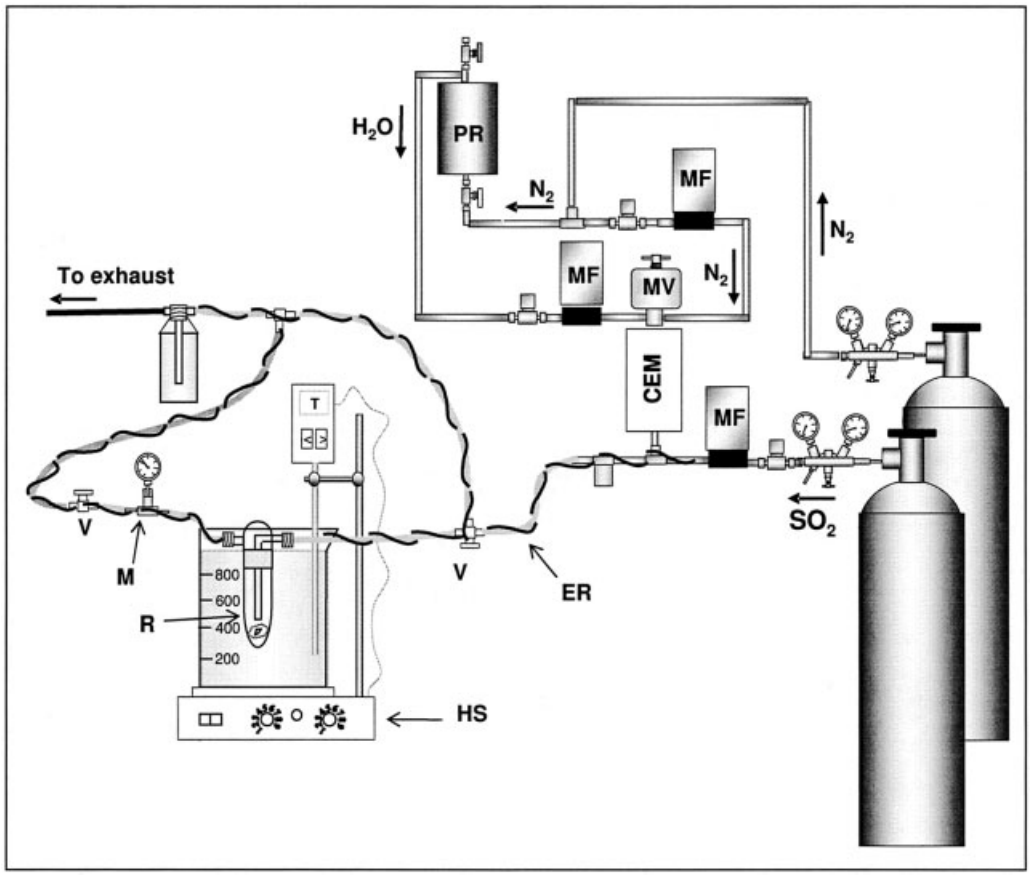

Figure 3. Experimental setup for TM-AFM experiments.

CEM: evaporator mixer chamber; ER: electric resistance; HS: heater stirrer; M: manometer; MF: mass flow-meter; PR: pressurized reservoir; R: reactor; V: valve.

Exploration of the reacted surfaces

The surface morphology of the reacted crystals either with or without a further humidification step was explored by TM-AFM (Extended MultiMode scanning probe Microscope Nanoscope IIIA, Digital Instruments, Santa Barbara, CA). The AFM probes were ultrasharp silicon tips (NT-MDT, Moscow, Russia) manufactured in single-crystal silicon with a nominal tip radius of 10 nm, pyramidal shape, a spring constant of 35 N/m, and a resonant frequency of 300 kHz. Furthermore, the sulfur distribution on the reacted samples was inspected by SEM equipped with energy-dispersive spectroscopy (EDS) microanalysis (Model JSM-840, operating at 10–15 kV; JEOL, Tokyo, Japan).

Results and Discussion

Evolution of surface morphology of reacted crystals after exposure to water vapor

The evolution of the morphology of $Ca(OH)_2$ (0001) surfaces—just after their attack by SO_2 and after further humidification according to procedures A, B, and C—is shown in Figures 4–7. In Figure 4, a $Ca(OH)_2$ (0001) plane is displayed just after being cleaved (Figures 4a1 and 4a2), after reaction with SO_2 at 50% RH (3.7 kPa) (Figures 4b1 and 4b2), and after a subsequent humidification period at 80% RH (5.9 kPa) (Figures 4c1 and 4c2) according to procedure A, in which all the regions were imaged quite close. A comparison between Figures 4b and 4c (before and after the humidification period) reveals a net change in the surface morphology induced by water vapor. The surface roughness increases from 8 to 21 nm and the largest features show a remarkable growth in height from 40 to 100 nm. The dramatic change in surface morphology might provide evidence of certain product crystal rearrangement on the $Ca(OH)_2$ (0001) planes induced by water vapor in such a way that product features might be grouped in clusters. As a result, larger product features would be built up. In fact, the phenomenon of crystal mobility on a surface was formerly reported by other researchers[22,23] for NaCl single crystals covered by $NaNO_{3(s)}$ product. Evidence of reorganization of $NaNO_3$ layers on NaCl surfaces into separate microcrystallites of $NaNO_3$ was provided by TEM imaging after exposure to a humid atmosphere (45–71% RH) at 295 K.[22] Moreover, a rearrangement of $NaNO_3$ layers to form well-defined $NaNO_3$ "towers" was also observed by AFM when a surface of a NaCl (100) single crystal previously attacked by dry HNO_3 was allowed to remain in contact with a water-saturated atmosphere.[23]

An extraordinary change in surface morphology induced by water vapor is also observed in Figure 5 for a $Ca(OH)_2$ (0001) plane just reacted at 30% RH (2.2 kPa) (see Figure 5a) and after

humidification for 3 and 6 days according to procedure B (see Figures 5b and 5c). An increase in surface roughness from 3 nm just after the SO_2 attack to 14–17 and 17–25 nm, respectively, after 3- and 6-day humidification periods is observed. It should be highlighted that no net change in terms of surface roughness is observed when imaging the sample after 9 and 17 days, which reflects that a final "steady-state" morphology seems to be reached after an approximately 6-day exposure to a humid atmosphere according to procedure B.

The TM-AFM images of a just-reacted $Ca(OH)_2$ (0001) surface after being kept in a dry atmosphere for 7 days (not shown here) did not reveal any change, with respect to either surface morphology or roughness. This observation reinforces the idea put forward that water is the active agent that promotes crystal rearrangement. Moreover, to ensure that this net change in the surface morphology arising from the action of water vapor is attributed only to the sulfite product [that is, $CaSO_3 \cdot (1/2)H_2O_{(s)}$] deposited on $Ca(OH)_2$ (0001), a cleaved and unreacted $Ca(OH)_2$ single crystal was subjected to humidification according to procedure B and imaged after 6 days. Inspection

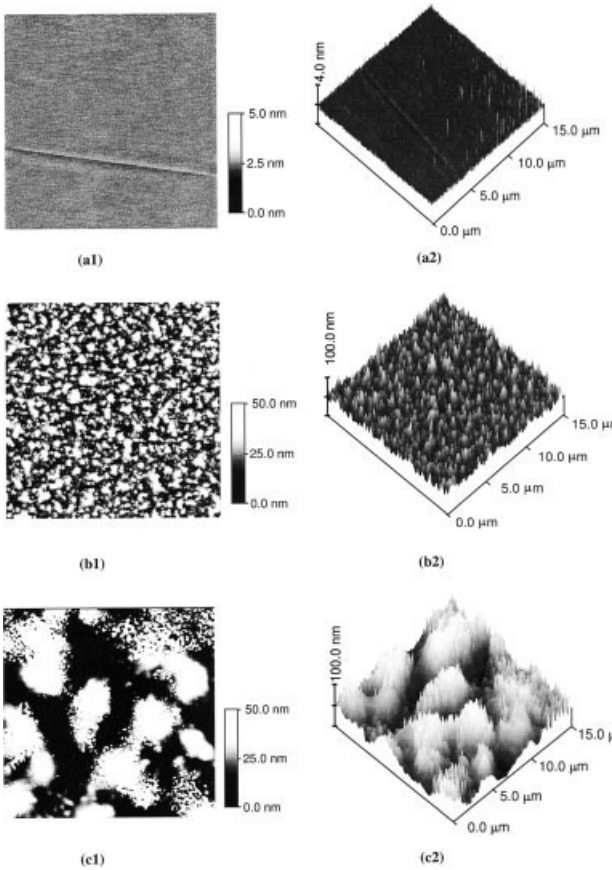

Figure 4. 2-D and 3-D 15 × 15 μm^2 TM-AFM images of a single-crystal $Ca(OH)_2$ (0001) surface reacted at 5500 ppm SO_2 concentration, 313 K, and 50% RH for 30 min and afterward humidified for 2 h at 313 K and 80% RH (procedure A).

(a) Freshly cleaved surface, Rms = 0.1 nm. (b) Surface just reacted, Rms = 7.8 nm. (c) Reacted surface after humidification, Rms = 20.7 nm.

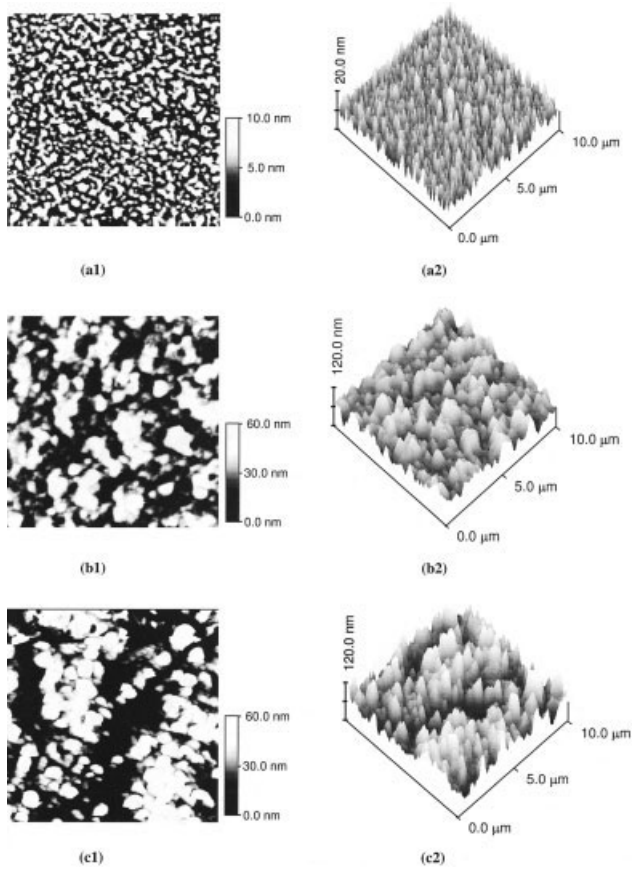

Figure 5. 2D and 3D 10 × 10 μm^2 TM-AFM images of a single-crystal $Ca(OH)_2$ (0001) surface reacted at 5500 ppm SO_2 concentration, 313 K, and 30% RH for 30 min and afterward under room conditions (288–298 K and 60–80% RH) (procedure B).

(a) Surface just reacted, Rms = 2.9 nm. (b) Reacted surface after 3 days, Rms = 14.4 nm. (c) Reacted surface after 6 days, Rms = 25.0 nm.

of the (0001) surface together with one of its profiles after the humidification period (see Figure 6) reveals the presence of small agglomerates or nodules up to 8 nm height and 0.5 μm width spread widely apart on the surface. It should be noted that this morphology differs from that shown in Figure 5c (obtained roughly after the same humidification period with procedure B), where larger features built up in a number of clusters can be observed. This result supports the idea that the aforementioned changes in the surface morphology might be mainly attributed to sulfite product rearrangement. On the other hand, if we assume that one layer of water has a thickness of about 0.25 nm,[24] the nodule features shown in Figure 6 cannot be related to water clusters or water islands because their size is too large. Consequently, formation of these nodules seems to be ascribed to a certain rearrangement of the $Ca(OH)_2$ (0001) surface, which might be caused by the presence of adsorbed water.

The evolution of surface morphology of a reacted sample at 30% RH (2.2 kPa), humidified according to procedure C, is

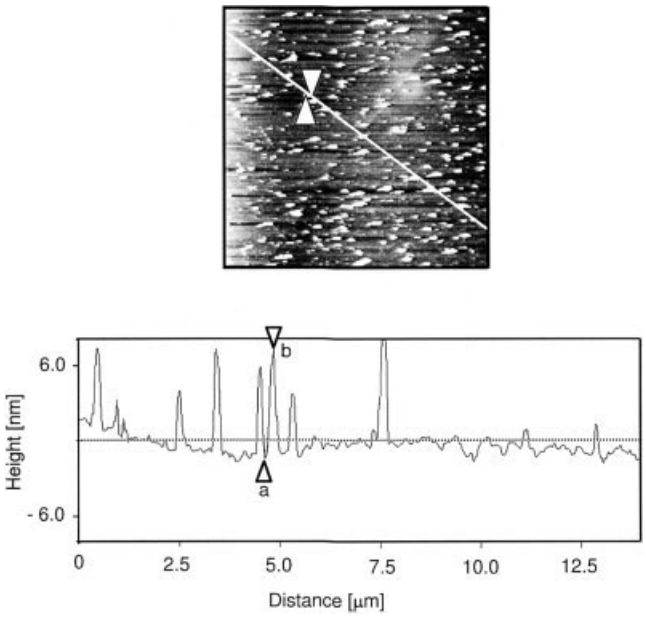

Figure 6. TM-AFM image of an unreacted single-crystal $Ca(OH)_2$ (0001) surface after exposure to a humid atmosphere at room conditions (288–298 K and 60–80% RH) (procedure B).

(a) 10×10 μm^2 image. (b) Profile.

shown in Figure 7. As can be seen in Figures 7a–7c, a nearly 7.5-min exposure of the sample to a humidified atmosphere causes an initial vertical growth of some features from 10 to 45 nm height with a slight increase of the surface roughness from 3.0 to 4.8 nm. However, a further relaxation of the surface can be observed in Figures 7d and 7e, which seems to indicate that this growth feature is unstable. The surface roughness (2.9 nm) is recovered after 10 min of humidification. Moreover, the images obtained during the following 90 min (not shown here) did not reflect any variation, in contrast to those obtained after 3 days (see Figure 7f), where a surface rearrangement similar to that visualized in Figures 4–6 was again observed. It should be noted that no remarkable changes in the surface morphology were observed for an unreacted cleaved $Ca(OH)_2$ single crystal treated according to procedure C.

Evidence of calcium sulfite aggregation

The AFM images shown in Figures 4, 5, and 7, obtained after humidification of some reacted samples using all the humidification procedures outlined above, provide evidence of certain crystal rearrangement on reacted $Ca(OH)_2$ (0001) planes induced by the action of water vapor. Furthermore, taking into account the humidification times and water partial pressures for procedures A, B, and C, water vapor also appears to play a role in the kinetics of the process. For procedure A (water vapor pressure: 5.9 kPa), clear changes on the surface were obtained after 120 min of humidification, whereas for procedure C, in which water vapor pressure was kept around 2.0 kPa, the surface was almost unchanged after 100 min. Therefore, once $Ca(OH)_2$ (0001) planes are almost covered by needle-like sulfite features after being attacked by SO_2, further humidification seems to promote crystal mobility and to allow crystal aggregation, which would be faster at higher vapor pressures. It should be noted that, in light of some previous experiments performed on commercial $Ca(OH)_2$ particles, the sulfite product appears to show chemical stability after at least 2 weeks.

Moreover, it could be assumed that the fresh active surface of $Ca(OH)_2$ might be generated as long as product aggregation takes place. To elucidate this point, some EDS elemental microanalyses were done on a $Ca(OH)_2$ (0001) surface reacted with SO_2 and subjected to further humidification. Given that the resolution of the technique is about 1 μm^3, a sample was prepared at experimental conditions that provided features of larger dimensions. Specifically, a $Ca(OH)_2$ single crystal was reacted at 50% RH (3.7 kPa) and humidified at 313 K and 80% RH (5.9 kPa) for 240 min according to procedure A.

A SEM micrograph of one large sulfite feature generated on a $Ca(OH)_2$ (0001) plane and the EDS spectra both in the center and in the surroundings of the feature are shown in Figure 8. As can be seen, the sulfur signal in the center of the feature is much higher than those obtained in its surroundings (see Figure 8b), which provides clear evidence of a preferential localization of the sulfite product in the feature. Impurities related to chlorine resulting from the $CaCl_2$ precursor of $Ca(OH)_2$ single-crystal preparation also show the same trend. This result sustains the assumption that water vapor enhances product mobility on $Ca(OH)_2$ (0001) planes. Following the idea advocated by Peters and Ewing,[9] water physically adsorbed on (0001) planes might form a nonrigid surface layer that would allow product crystallites to diffuse by the formation of H-bonds to subsequently generate larger features. A schematic representation of the feature rearrangement process on $Ca(OH)_2$ (0001) after exposure to a highly humid atmosphere is illustrated in Figure 9.

Proposal of a reaction mechanism

A reaction mechanism that might be consistent with the experimental observation that water vapor induces sulfite rearrangement and a net change in surface morphology of $Ca(OH)_2$ (0001) single crystals attacked by SO_2 after exposure to a humid atmosphere might consist of the following steps (see Figure 10):

1. Water adsorption. Water might adsorb on $Ca(OH)_2$ (0001) planes to form a physically adsorbed water multilayer at high RH (see Figure 10a). This multilayer might show a "liquid-like" behavior at surface coverage > 2, which might be achieved at high RH values according to Klingspor et al.[7]

2. Hydration of SO_2. Hydration of SO_2 by adsorbed water molecules could occur to form $SO_2 \cdot zH_2O_{(ads)}$ complexes (see Figure 10b), as was also suggested by Klingspor et al.[7] This step is sustained by the general tendency of SO_2 to be hydrated both in the gas phase[25] and in the liquid phase,[26] which might be reinforced by the expected quasi-liquid nature of the water multilayer on hydrophilic $Ca(OH)_2$ (0001) planes.

3. Reaction of $SO_2 \cdot zH_2O$ complexes with $Ca(OH)_2$ to generate "needle-like" $CaSO_3 \cdot (1/2)H_2O$ features. Two different pathways can be suggested:

3.1. *Solvation of Ca^{2+} and HO^- ions and product precipitation*. According to Peters and Ewing,[9] this mechanism involves a partial dissolution of $Ca(OH)_2$ on the adsorbed water

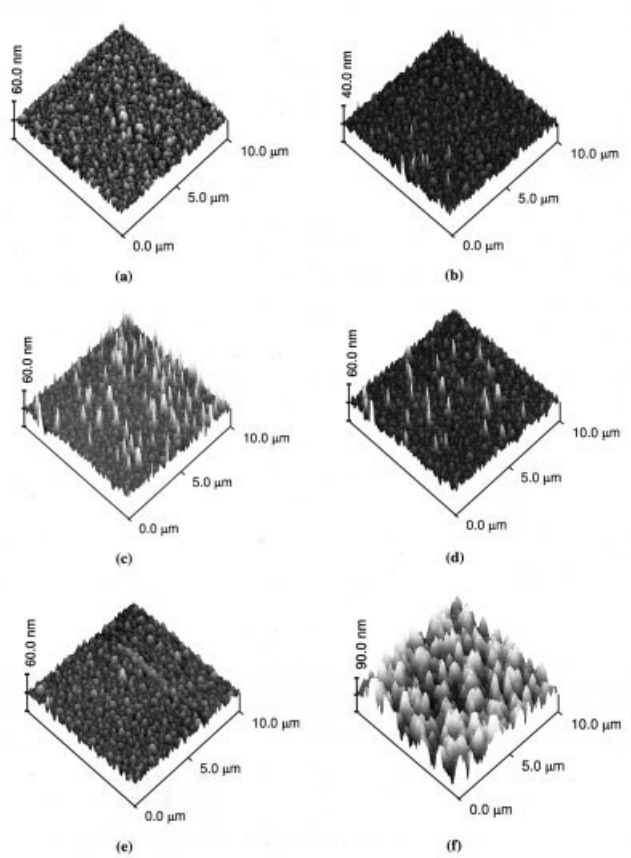

Figure 7. TM-AFM images (10 × 10 μm^2) of the temporal evolution of a crystal surface reacted at 5500 ppm SO_2 concentration, 313 K, and 30% RH for 30 min placed in a controlled humidity chamber at 293 K (procedure C).

The time and RH variation of each image is shown in the accompanying scheme. Rms (in nm): (a) 3.0; (b) 3.0; (c) 4.8; (d) 3.6; (e) 2.9; (f) 17.1.

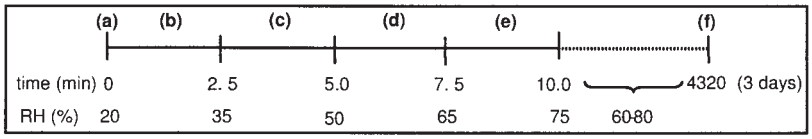

multilayer with the formation of solvated Ca^{2+} and HO^- ions. The reaction would then take place between solvated HO^- ions and $SO_2{\cdot}zH_2O_{(ads)}$ complexes with the formation of solvated SO_3^{2-} ions, which might subsequently precipitate with Ca^{2+} ions resulting from saturation of the adsorbed water multilayer.

3.2. *Solid-state mechanism*. This mechanism involves a direct interaction between $SO_2{\cdot}zH_2O_{(ads)}$ complexes and lattice Ca^{2+} and HO^- ions on $Ca(OH)_2$ (0001) planes. Because Ca^{2+} and HO^- ions occupy fixed positions in the $Ca(OH)_2$ crystalline lattice, only some orientations of $SO_2{\cdot}zH_2O$ complexes with respect to the crystal are expected to be reactive. The projection of the (0001) plane for two $Ca(OH)_2$ unit cells is illustrated in Figure 10c. On the basis of the ionic radius of Ca^{2+} ions (0.99 Å[27]) and the $Ca(OH)_2$ lattice parameters (see Table 1), and the requirement of orientation of the S—O dipole, $SO_2{\cdot}zH_2O$ complexes (kinetic diameter $\gg$ 5.0 Å for the coordination of more than two water molecules to SO_2[25]) are expected to react with Ca^{2+} and HO^- (0001) ions only along a tangential direction ("tangential attack or etching") (see Figure 10c). According to geometrical reasons, only molecules up to 3.4 Å in size [distance between two Ca^{2+} ions placed along the diagonal in a Ca layer of a $Ca(OH)_2$ unit cell; see Figure 1a] might be allowed to cross a layer of Ca^{2+} ions. Subsequently, $SO_2{\cdot}zH_2O$ complexes might proceed to the formation of a covalent bond between the sulfur and the oxygen atom of a HO^- (0001) ion, thus leading to a new complex. The remaining proton in this complex might be stabilized by another HO^- (0001) ion released from the lattice through H-bonding with the ultimate formation of one H_2O molecule, which would stoichiometrically equal the overall reaction (Eq. 1). Eventually, a new $CaSO_3{\cdot}(1/2)H_2O_{(s)}$ crystal would be formed from the interaction of the final complex with a Ca^{2+} (0001) ion.

In a comparison of both mechanisms, ion dissolution and precipitation appear to be thermodynamically less favored because: (1) $Ca(OH)_2$ is very insoluble (Kps = 5.02 × 10^{-6}), which makes it extremely difficult to dissolve a sufficient number of HO^- and Ca^{2+} ions in the adsorbed water multi-

layer covering the $Ca(OH)_2$ (0001) planes to account for the observed experimental sulfur uptake values[16]; and (2) it requires high water coverage to allow the presence of water multilayers, which, according to the adsorption isotherm of water on $Ca(OH)_2$,[7] occur only at very high RH values. Furthermore, this mechanism would likely involve the formation of an amorphous rather than a crystalline product, which is in disagreement with the XRD patterns obtained for reacted commercial $Ca(OH)_2$ particles (not shown here).

It is well known that the surface morphology of a solid is crucial in the progress of solid-state reactions, where the reactivity of a species is often determined by its arrangement on particular planes of a crystal rather than by its intrinsic chemical reactivity.[28] Moreover, it should be emphasized that regions with high density of defects (such as steps and kinks) in a reactive plane are energetically more favorable than terraces to establish interactions with adsorbed molecules. Regarding the reaction between SO_2 and $Ca(OH)_2$ (0001), because the attack seems to be preferentially tangential, the presence of defects (presumably steps according to Figure 2) might be relevant to account for the progress of the reaction. Furthermore, a role of defects could also explain the dispersion in the surface roughness found in different regions of $Ca(OH)_2$ (0001) single crystals attacked by SO_2 at high RH reported in our previous AFM study,[15] which might involve the presence of crystalline domains of different reactivity.

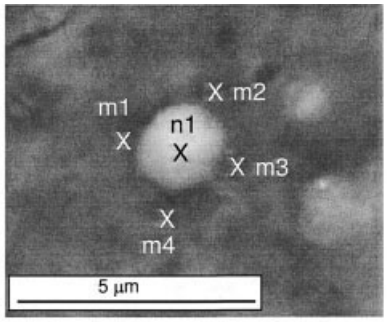

(a)

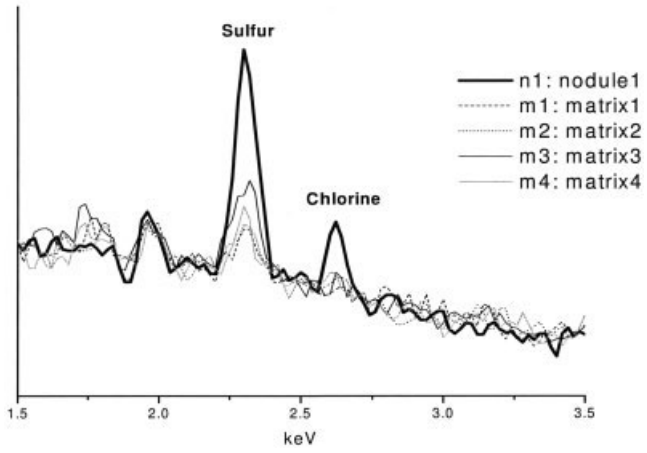

Figure 8. SEM and EDS analyses of a crystal reacted at 5500 ppm SO_2 concentration, 313 K, and 50% RH for 30 min and after being humidified at 313 K and 80% RH for 4 h.

(a) SEM micrograph of one large feature (n and m denote the feature and its surroundings, respectively). (b) EDS elemental spectra, where it can be seen that a higher amount of sulfur is localized in the feature.

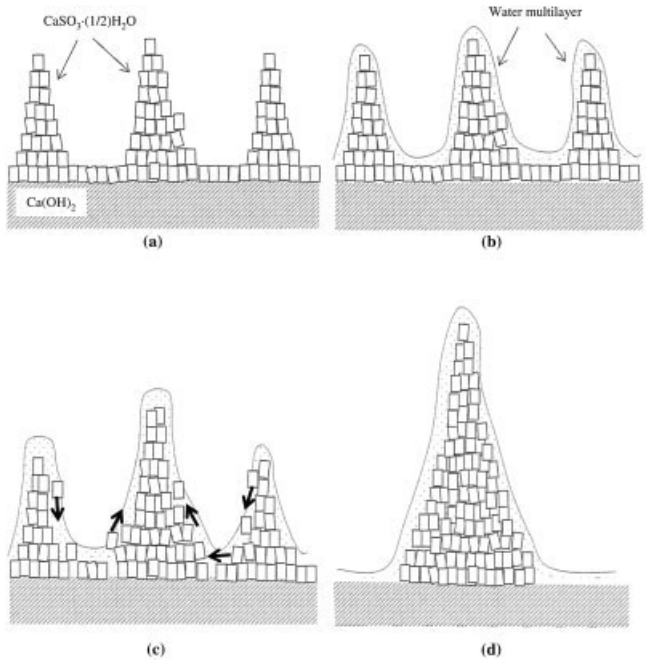

Figure 9. Schematic representation of the evolution of $CaSO_3 \cdot (1/2)H_2O$ "needle-like" features onto a single-crystal $Ca(OH)_2$ (0001) surface when it comes into contact with a high water vapor pressure atmosphere.

(a) Close needle-like features of $CaSO_3 \cdot (1/2)H_2O$. (b) Water adsorption on $CaSO_3 \cdot (1/2)H_2O$ crystallites. (c) Diffusion of $CaSO_3 \cdot (1/2)H_2O$ crystallites by the interaction with water molecules. (d) "Cluster-like" feature morphology.

4. Diffusion of product crystallites and surface rearrangement. The exposure of the "needle-like" $CaSO_3 \cdot (1/2)H_2O$ features to a humid atmosphere would involve the removal of a number of product crystallites from their initial positions and further diffusion on the $Ca(OH)_2$ (0001) planes to aggregate with other crystallites, with the subsequent formation of larger needle-like features in a cluster-like configuration. This crystallite diffusion, which seems to be subjected to the presence of adsorbed water, might liberate or open up a new surface of $Ca(OH)_2$ for further reaction, as discussed earlier.

The rearrangement of the surface toward the formation of a cluster-like morphology could be regarded as a stressing phenomenon of the surface, which would therefore require the supply of free energy. The consecutive elementary steps involved in the reaction mechanism could provide the required free energy in a different way. First, on the grounds of its exothermic character, the adsorption of water for surface coverage > 1.0 (see Figure 10a) could contribute to such free energy. To our knowledge, no data for adsorption enthalpies of water on $Ca(OH)_2$ have been reported in the literature. However, for the water–NaCl system,[9] an experimental adsorption

enthalpy of about -42 kJ mol^{-1} has been reported for the range 1.0–3.0 of surface coverage, which is very close to the enthalpy of condensation of water vapor. Because this latter value is irrespective of the solid nature for high surface coverage, this result might also be taken into account for the system $H_2O/Ca(OH)_2/CaSO_3$. Furthermore, the SO_2 hydration (see Figure 10b), also regarded as an exothermic step, might supply part of the required free energy. However, given that crystallite diffusion has been clearly stated by several humidification procedures after the reaction (that is, in the absence of SO_2), the exothermic character of the hydration process cannot of itself explain this phenomenon. For the same reason, the thermodynamics of the reaction between $SO_2 \cdot zH_2O$ and $Ca(OH)_2$ (see Figure 10c) do not either seem to be crucial to explain such crystal rearrangement.

Mechanistic implications on the kinetics of sulfur uptake by hydrated lime

The concept "surface deactivation"—defined and applied in our description of the kinetics of the desulfurization reaction[16,17]—might also be related to the surface mechanism described above. In this way, the evidence of crystallite rearrangement on $Ca(OH)_2$ (0001) planes with the humidification of samples after being attacked by SO_2 might account for the dramatic enhancement of the reactivity observed for commercial $Ca(OH)_2$ particles with the RH in FGD technologies, in terms of both sulfur uptake and reaction rate. Accordingly, an increase of the RH might enhance the surface diffusion of sulfite crystallites on $Ca(OH)_2$, thus providing a lower surface deactivation.

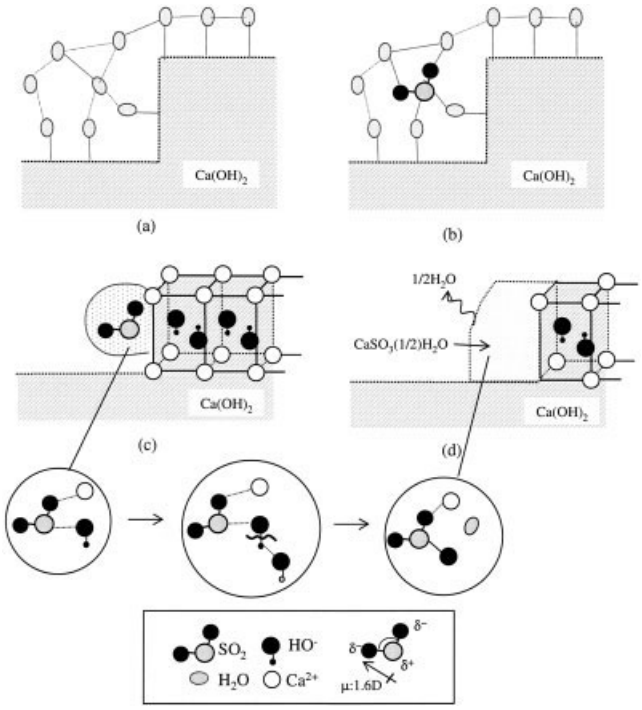

Figure 10. Reaction mechanism proposed for the desulfurization reaction.

(a) Water adsorption on the surface of $Ca(OH)_2$. (b) Formation of $SO_2 \cdot zH_2O$ complex. (c) Orientation of SO_2 complex on the surface in such a way that the sulfur interacts with HO^- ions and the oxygen interacts with Ca^{2+} ions and the subsequent formation of a complex. (d) Formation of $CaSO_3 \cdot (1/2)H_2O$ from the latter complex, formation of $(1/2)H_2O$ molecule and reaction of one H^+ ion released from the complex and one HO^- released from the lattice.

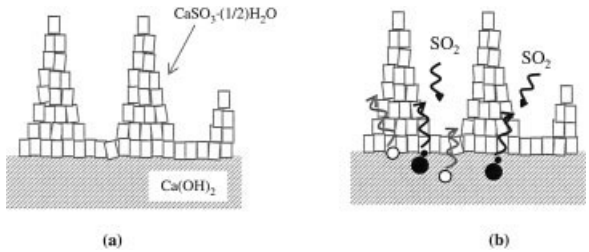

Figure 11. Outward ionic solid-state diffusion mechanism.

(a) Deactivated surface. (b) Ca^{2+} and HO^- ionic outward solid-state diffusion, where the ions attaining the surface can react with SO_2.

Furthermore, the experimental observation that the reaction between hydrated lime and SO_2 does not stop after long periods of time (>1 h)[16] and that it progresses at very low reaction rates can also be accounted for by the mechanism described above. After a long-time exposure to SO_2, the surface of commercial hydrated lime might show a high degree of deactivation, that is, no further active surface of $Ca(OH)_2$ would be accessible for SO_2 attack because crystallite diffusion, which would provide free or new $Ca(OH)_2$ surface for further reaction, might decline with time. In this situation, the reaction might proceed according to the following pathways:

(1) *Ionic outward solid-state diffusion*. Because the reagent surface is partially deactivated, SO_2 might continue to react with Ca^{2+} and HO^- ions from the crystalline lattice of $Ca(OH)_2$ that attain the outer surface by diffusion from the $Ca(OH)_2/CaSO_3 \cdot (1/2)H_2O$ to the outer surface (see Figure 11). We included this step in a modified deactivation kinetic model (DM-ISCM),[16] which allowed a better description of our kinetic experimental data. The outward ionic diffusion process might be promoted in the grain boundaries between adjacent $CaSO_3 \cdot (1/2)H_2O$ crystallites as a result of the action of adsorbed or even condensed water arising from capillary forces, especially HO^- ion diffusion, where a mechanism based on H^+ transfer between water molecules with an inward direction can be proposed.[25]

(2) *Residual active surface*. In this case, a final steady state is assumed, where the rates of removal and formation of product crystallites on the reagent surface might be similar, but very low, as schematically represented in Figure 12. As a result, the reagent surface might show a number of partially deactivated or residual areas where the desulfurization reaction could occur, but at very low rates.

Both pathways would be consistent with a number of studies in the literature that report no dependency of the reaction rate with SO_2 concentration at long periods of time (after a few minutes). Meanwhile, however, the rate of the ionic outward solid-state diffusion pathway is controlled by an ionic diffusion process, and the residual active surface pathway must be limited by the rate of product removal from the surface. No experimental evidence has been found to discern between both

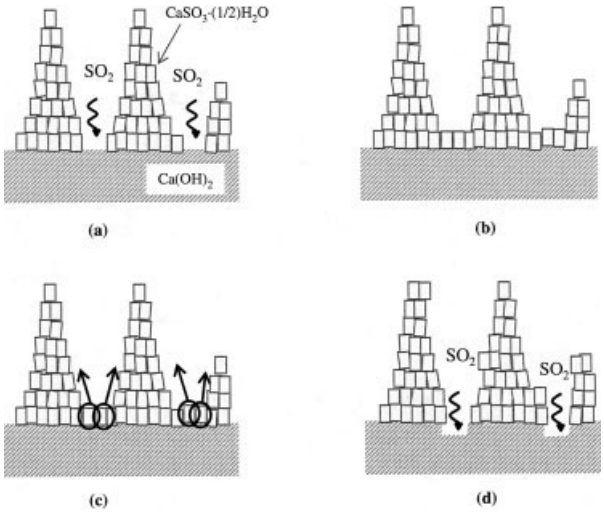

Figure 12. Residual active surface mechanism.

(a) Residual active surface, which can react with SO_2. (b) $CaSO_3 \cdot (1/2)H_2O$ formation. (c) Removal of product crystals from the surface by diffusion. (d) New generation of residual active surface.

pathways. Although both of them might take place simultaneously, the prevailing one might depend on the ratio between the rate at which crystal product is removed from the surface and the reaction rate. It could be suggested that the ionic solid-state diffusion pathway might govern the reaction at lower ratios, whereas the former might do so at ratios tending to unity.

Conclusions

The AFM technique constitutes a useful tool for the visualization of the reaction between SO_2 and $Ca(OH)_2$ single crystals at low temperature. A substantial change in the surface morphology of $Ca(OH)_2$ (0001) surface attacked by SO_2 is observed after being in contact with a humid atmosphere, where sulfite needle-like features are grouped in clusters that open up new and fresh surfaces susceptible to further reaction with SO_2. Water physically adsorbed on the surface of $Ca(OH)_2$ (0001), especially when forming multilayers, might play a role in all four mechanistic steps suggested in this work. These morphology changes are regarded as crucial to understand the role of water in the reaction and its mechanistic implications on the kinetics of the desulfurization reaction. The widely reported experimental observation concerning the crucial influence exerted by the relative humidity (RH) on the ability of the $Ca(OH)_2$ to retain SO_2 might be ultimately attributed to the phenomenon of crystallite reorganization. For the case of "real-life" surface conditions in FGD applications, the phenomenon of crystal rearrangement might also be combined with other phenomena such as pore-mouth plugging or pore filling that could also take place on real particles.

Acknowledgments

The authors are thankful to Drs. J. Diaz and I. Diaz-Perez of the group of Nanometric Techniques at the Serveis Cientifico-Tecnics (University of Barcelona) for assistance in carrying out the AFM explorations. The authors thank Comisión Interministerial de Ciencia y Tecnología of Spain (Projects AMB94-0200 and QUI98--0361) for funding.

Literature Cited

1. Manahan SE. *Environmental Chemistry*. 6th Edition. Boca Raton, FL: Lewis; 1994.
2. Jorgensen C, Chang JCS, Brna TG. Evaluation of sorbents and additives for dry SO_2 removal. *Environ Prog.* 1987;6:26-32.
3. Dahlin R, Vann Busch P, Snyder T. Literature review and assembly of theories on the interactions of ash and FGD sorbents. Report prepared by Southern Research Institute, Birmingham, AL for the U.S. Department of Energy of Pittsburgh Energy Technology Center; 1992.
4. Krammer G, Brunner Ch, Khinast J, Staudinger G. Reaction of $Ca(OH)_2$ with SO_2 at low temperature. *Ind Eng Chem Res.* 1997;36: 1410-1418.
5. Karatepe N, Ersoy-Meriçboyu A, Yavuz R. Kinetic model for desulfurization at low temperatures using hydrated sorbent. *Therm Acta*. 1999;127-134.
6. Garea A, Herrera JL, Renedo MJ, Fernandez J, Irabien AJ. Thermogravimetric determination of the influence of water vapor in the FGD in-duct injection at low temperatures. *Chem Technol Biotechnol.* 2000; 75:484-490.
7. Klingspor J, Strömberg AM, Karlsson HT, Bjerle I. Similarities between lime and limestone in wet-dry scrubbing. *Chem Eng Process.* 1984;18:239-247.
8. Beruto DT, Botter R. Liquid-like H_2O adsorption layers to catalyze the $Ca(OH)_2/CO_2$ solid–gas reaction and to form a non-protective solid product layer at 20°C. *J Eur Ceram Soc.* 2000;20:497-503.
9. Peters SJ, Ewing EJ. Water on salt: An infrared study of adsorbed H2O on NaCl(100) under ambient conditions. *J Phys Chem B.* 1997;101: 10880-10886.
10. Foster MC, Ewing GE. Adsorption of water on the NaCl(001) surface. II. An infrared study at ambient temperatures. *J Chem Phys.* 2000; 112:6817-6826.
11. Engkvist O, Stone AJ. Adsorption of water on the NaCl(001) surface. III. Monte Carlo simulations at ambient temperature. *J Chem Phys.* 2000;112:6827-6833.
12. Damle AS, Ramanathan K, Harmon DL. Kinetics of reaction between hydrated lime and sulfur dioxide. Vol. 1. Proceedings of the 6th Symposium of Transfer Utility Control Technology, EPRI CS-4918; 1986.
13. Weinell CE, Jensen PI, Dam-Johansen K, Livbjerg H. Hydrogen chloride reaction with lime and limestone: Kinetics and sorption capacity. *Ind Eng Chem Res.* 1992;31:164-171.
14. Rochelle GT, Jozewicz W. Reaction of hydrated lime with SO_2 in humidified flue gas. Proceedings of SO_2 Control Symposium, New Orleans, LA, May; 1990.
15. Bausach M, Pera-Titus M, Tejero J, Cunill F. AFM observation of $Ca(OH)_2$ (0001) surfaces reacted with SO_2: Role of water vapour on product morphology. *Chem Lett.* 2006;35:24-25.
16. Bausach M, Pera-Titus M, Fite C, Cunill F, Izquierdo J-F, Tejero J, Iborra M. Kinetic modeling of the reaction between hydrated lime and SO_2 at low temperature. *AIChE J.* 2005;51:1455-1466.
17. Bausach M, Pera-Titus M, Fite C, Cunill F, Izquierdo J-F, Tejero J, Iborra M. Enhancement of gas desulfurization with hydrated lime at low temperature by the presence of NO_2. *Ind Eng Chem Res.* 2005; 44:9040-9049.
18. Brauer G. *Quimica Inorganica Preparative*. Barcelona, Spain: Reverte; 1958.
19. Pauling L. *The Nature of the Chemical Bond and the Structure of Molecules and Crystals: An Introduction to Modern Structural Chemistry*. 3rd Edition. Ithaca, NY: Cornell Univ. Press; 1960.
20. Moreno JA, Mizrachi S, Oppeltz V. Proton dynamics in calcium hydroxide. A NMR study. *Solid State Commun.* 1984;51:597-601.
21. Chaix-Pulchery O, Pannetier J, Bouillot J, Niepce JC. Structural prereactional transformations in $Ca(OH)_2$. *J Solid State Chem.* 1987;67: 225-234.
22. Allen HC, Laux JM, Vogt R, Finlayson-Pitts BJ, Hemminger JC. Water-induced reorganization of ultrathin nitrate films on NaCl: Implications for the tropospheric chemistry of sea salt particles. *J Phys Chem.* 1996;100:6371-6375.

23. Zangmeister CD, Pemberton JE. In-situ monitoring of the NaCl + HNO_3 surface reaction: The observation of mobile surface strings. *J Phys Chem B.* 1998;102:8950-8953.
24. Cantrell W, Ewing GE. Thin film water on muscovite mica. *J Phys Chem B.* 2001;105:5434-5439.
25. Loerting T, Kroemer RT, Liedl KR. On the competing hydrations of sulfur dioxide and sulfur trioxide in our atmosphere. *Chem Commun*. 2000:999-1000.
26. Greenwood NN, Earnshaw A. *Chemistry of the Elements*. Oxford, UK: Pergamon Press; 1986.
27. Levine IN. *Physical Chemistry*. 2nd Edition. New York, NY: McGraw-Hill; 1983.
28. Rao CNR, Gopalakrishnan J. *New Directions in Solid State Chemistry*. 2nd Edition. Cambridge, UK: Cambridge Univ. Press; 1997.

Manuscript received Jan. 17, 2006, and revision received Apr. 28, 2006.